

Structures and Properties of $\text{LaFe}_{0.8}\text{Cu}_{0.2}\text{O}_{3-\delta}$ and $\text{BaFe}_{0.8}\text{Cu}_{0.2}\text{O}_{3-\delta}$ as Cobalt-Free Perovskite-Type Cathode Materials for the Oxygen Reduction Reaction

Asim Idrees,^[a] Xuening Jiang,^{*[a]} Gang Liu,^[a] Hao Luo,^[a] Guoqiang Jia,^[a] Qingyu Zhang,^[a] Lei Jiang,^[b] Xiangnan Li,^[c] and Baomin Xu^[c]

Perovskite oxides with mixed electronic–ionic conduction are important catalysts for the oxygen reduction reaction in solid oxide fuel cells (SOFCs). Here, two cobalt-free perovskite oxides, $\text{LaFe}_{0.8}\text{Cu}_{0.2}\text{O}_{3-\delta}$ (LFCuO) and $\text{BaFe}_{0.8}\text{Cu}_{0.2}\text{O}_{3-\delta}$ (BFCuO), were synthesized and comparatively studied with respect to their phase structures, oxygen contents, chemical defects, thermal expansion coefficient (TEC), as well as electrical and electrochemical properties. Different structures and properties have been found for each oxide, which have been interpreted

based on their tolerance factors and chemical defects. LFCuO showed much better overall performance than BFCuO, and it proved to be a promising cobalt-free cathode material of intermediate-temperature SOFCs with a low TEC ($12.0 \times 10^{-6} \text{ }^\circ\text{C}^{-1}$) that matches well with TECs of the electrolytes, high catalytic activity for the oxygen reduction reaction characterized by low area specific resistances ($0.090 \text{ } \Omega \text{ cm}^2$ at $800 \text{ }^\circ\text{C}$ and $0.20 \text{ } \Omega \text{ cm}^2$ at $750 \text{ }^\circ\text{C}$), and high-temperature chemical stability with electrolytes.

1. Introduction

Perovskite-type oxides with mixed ionic–electronic conduction are used in catalysis and electrocatalysis, and they are of particular interests for technologies of catalytic combustion, catalytic reduction of CO_2 , water splitting, solid oxide fuel cells (SOFCs), and solid oxide electrolysis cells (SOECs).^[1–5] As cathode materials of SOFC devices, perovskite oxides should have high catalytic activity for the oxygen reduction reaction (ORR) at temperatures of $500\text{--}800 \text{ }^\circ\text{C}$ (intermediate temperature, IT), low thermal expansion coefficients (TECs) that match well with other component materials, and good chemical stability at high temperatures. These properties are closely associated

with the composition, phase structure, and chemical defects of the oxides.^[6,7]


Cobalt-based perovskite oxides, such as cubic perovskite oxide of $\text{La}_{0.5}\text{Sr}_{0.5}\text{CoO}_{3-\delta}$ ^[8] and double-layered perovskite oxides of $\text{LnBaCo}_2\text{O}_{5+\delta}$ (Ln = lanthanum),^[9,10] are important candidate cathode materials for SOFCs. The interchangeable valence states of Co^{n+} ($n = 2, 3, 4$) ions contribute to the high ORR catalytic activity of these oxides, which, however, can also cause high TEC values ($> 20 \times 10^{-6} \text{ }^\circ\text{C}^{-1}$) that are much larger than the TECs of commonly used electrolytes, $(11\text{--}13) \times 10^{-6} \text{ }^\circ\text{C}^{-1}$.^[11–13] Such thermal expansion mismatching between the component materials can cause structural cracking and performance degradation of SOFCs during the long-term working period and the high-temperature fabrication process of the cell.^[7] Furthermore, volatility of these cobalt-based oxides at elevated temperatures and the relatively high price of cobalt also limit their practical application as cathode materials in IT-SOFCs. Thus, the development of Co-free perovskite-type cathodes has been receiving growing interest in recent years.^[14–17]


As a typical Fe-based cobalt-free perovskite oxide, $\text{BaFeO}_{3-\delta}$ proved to be a promising cobalt-free cathode material of IT-SOFCs with high surface exchange kinetics and high ORR electrocatalytic activity.^[15] However, owing to its large Goldschmidt tolerance factor ($\tau = 1.006$),^[18] a single cubic phase $\text{BaFeO}_{3-\delta}$ could not be obtained at room temperature with various synthesis methods, such as solid-state and sol-gel reactions, and more complicated fabrication methods are required to obtain such a pure phase.^[15,18,19] To stabilize the cubic structure of $\text{BaFeO}_{3-\delta}$, A-site and/or B-site doping has been adopted,^[18–20] but the new oxides still have problems with either low ORR catalytic activity or large TECs that mismatch with the electrolyte. As a result, to improve the overall performance of

[a] A. Idrees, Prof. X. Jiang, G. Liu, H. Luo, G. Jia, Q. Zhang
Key Laboratory of Materials Modification by Laser, Ion, and
Electron Beams (Ministry of Education), School of Physics
Dalian University of Technology
No. 2 Linggong Road, Ganjingzi District, Dalian, 116024 (P. R. China)
E-mail: xnjiang@dlut.edu.cn

[b] Prof. L. Jiang
Dalian Institute of Chemical and Physics, CAS
457 Zhongshan Road, Dalian, 116023 (P. R. China)

[c] Dr. X. Li, Prof. B. Xu
Department of Materials Science and Engineering
Southern University of Science and Technology
Shenzhen, 518055 (P. R. China)

 The ORCID identification number(s) for the author(s) of this article can be found under:
<https://doi.org/10.1002/open.201800097>.

 © 2018 The Authors. Published by Wiley-VCH Verlag GmbH & Co. KGaA. This is an open access article under the terms of the Creative Commons Attribution-NonCommercial-NoDerivs License, which permits use and distribution in any medium, provided the original work is properly cited, the use is non-commercial and no modifications or adaptations are made.

BaFeO_{3-δ} as a cathode material for IT-SOFCs, the phase structure and properties, especially the electrochemical performance and TEC value, should be well balanced by tailoring the A-site and/or B-site dopant.

In this work, La³⁺ substitution at A sites and Cu²⁺ doping at B sites were adopted in BaFeO_{3-δ} for both property modifications and to understand the effects of A-site and B-site cations on the structure and properties of the perovskite oxide. Cu²⁺ was chosen as the B-site dopant because of its smaller ionic radius than Fe³⁺ to give a smaller tolerance factor of the oxide, its stable oxidation state against thermal reduction, as well as its ability to enhance oxygen surface adsorption and bulk diffusion for the cathodes.^[16,21,22] Besides, La³⁺, with a different ionic radius and valence state to Ba²⁺ at A sites, is expected to have synergetic effects on both the structure and the properties of BaFeO_{3-δ}. Two perovskite oxides, BaFe_{0.8}Cu_{0.2}O_{3-δ} (BFCuO) and LaFe_{0.8}Cu_{0.2}O_{3-δ} (LFCuO), were synthesized and comparatively studied as cathode materials for IT-SOFCs. Different structures and properties have been found for them, which are interpreted based on the results of the tolerance factor, oxygen content, and chemical defects of the oxides. More significantly, LFCuO proves to be a promising cathode material for IT-SOFCs with high catalytic activity for the ORR and a low TEC value that perfectly matches with the electrolyte materials.

2. Results and Discussion

2.1. Phase Structures

Figure 1 shows XRD patterns of the synthesized BFCuO, LFCuO, and Ba-Fe-O powders, which were indexed with different phase structures. The BFCuO pattern was well indexed with a cubic perovskite structure (*Pm-3m* space group) with a lattice parameter of $a = 4.062 \text{ \AA}$. This structure, as illustrated in Figure 1, has ideal BO₆ octahedrons with Fe and Cu²⁺ sharing the B site and Ba²⁺ at A site. BFCuO is the BaFeO₃ oxide with

20 mol% Fe ions at B sites replaced by Cu²⁺. It was previously reported^[15,18] that the cubic perovskite structure of BaFeO₃ was not stable at room temperature, owing to a large Goldschmidt tolerance factor ($\tau > 1$) and could only exist at high temperatures above 900 °C. Similar results were obtained with the EDTA sol-gel synthesis method in this work. As shown in Figure 1, the sample for the composition of BaFeO₃ was composed of a mixture of Ba-Fe-O oxides with various phase structures at room temperature. However, the BFCuO oxide synthesized under the same conditions was a pure phase, indicating that B-site Cu²⁺ doping significantly improved the stability of the cubic perovskite structure of BaFeO₃.

When the A-site cations were changed from Ba²⁺ to La³⁺, the phase structure of the oxide changed as well. In contrast to the cubic perovskite structure of BFCuO, the diffraction peaks of LFCuO were indexed with an orthorhombically distorted perovskite structure with space group of *Pnma* (ICSD 88–0641). This structure, as reported for LaFeO₃,^[23] can be represented by the Glazer tilt system of $a^+b^-b^-$ characteristic of tilting BO₆ octahedrons, which gives rise to an enlarged unit cell relative to the pseudocubic perovskite cell (lattice parameter of a_p) given by $a_0 \approx a_p$, $b_0 \approx 2a_p$ and $c_0 \approx a_p$ in the *Pnma* structure. As demonstrated by Woodward,^[24] a balance of favorable covalent versus ionic bonding interactions at the A sites is largely responsible for this *Pnma* particular distortion. This may explain, in part, the different phase structures between LFCuO and BFCuO, as they have different A-site cations. In addition, the perovskite structure is also closely related to Goldschmidt tolerance factor (τ) of the oxide.^[25] The tolerance factors of LFCuO and BFCuO were calculated based on the ionic radius from Shannon (1976) and the results are listed in Table 1. The τ value is very close to 1 for BFCuO, which explains its cubic perovskite structure. However, τ is only 0.876 for LFCuO, and this value is just within the τ range for the *Pnma*-type distorted perovskite structure.^[25] This further explains the different phase structures of the BFCuO and LFCuO oxides.

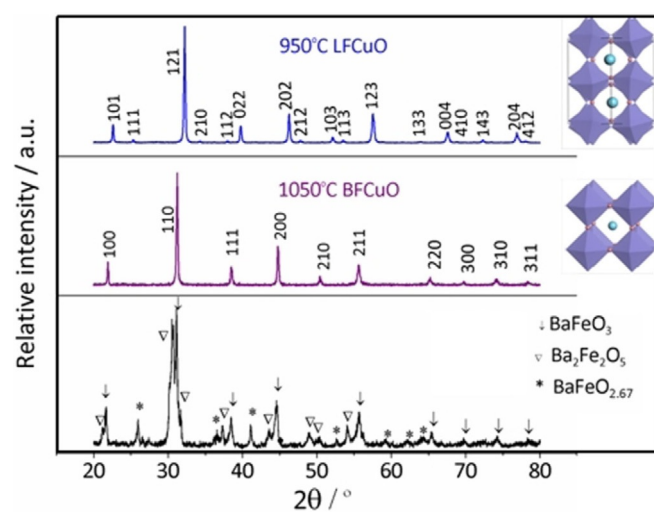


Figure 1. XRD patterns of the synthesized BFCuO, LFCuO, and Ba-Fe-O powders with the corresponding schematic phase structures.

Sample	Space group	Lattice parameter [Å]	Cell volume [Å ³]	Tolerance factor (τ)	3- δ	δ	n
LFCuO	<i>Pnma</i>	5.547 (a) 7.888 (b) 5.563 (c)	243.43	0.876	2.98	0.020	3.21
BFCuO	<i>Pm-3 m</i>	4.062	67.02	0.979	2.60	0.40	3.49

2.2. Thermal Expansion Behaviors

A cathode material for a SOFC should have a proper TEC value that matches the TECs of the electrolyte materials in order to maintain structural and performance stability of the cells.^[7] Thermal expansion curves of BFCuO and LFCuO oxides were measured at 25–900 °C in air, and the results are shown in Figure 2. Different expansion behaviors were observed for

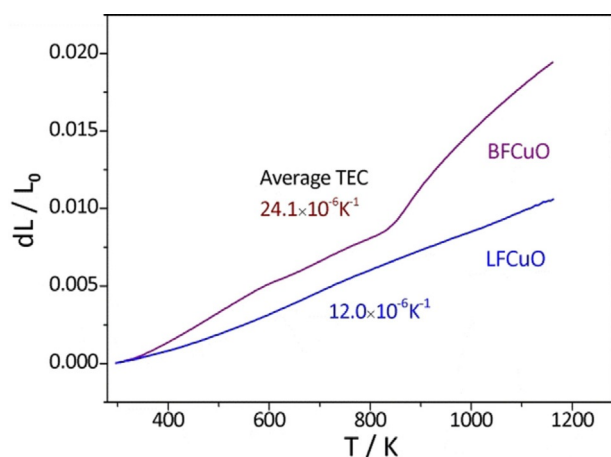


Figure 2. Thermal expansion curves of BFCuO and LFCuO measured at 25–900 °C in air with the corresponding average TEC values.

these samples. In the expansion curve of BFCuO, an inflection was observed at 570 °C, which could be ascribed to reduction of Fe^{4+} to Fe^{3+} , caused by the thermally driven release of lattice oxygen, as found in other perovskite oxides.^[26,27] Different slopes of the curve in the low- and high-temperature ranges gave rise to different TEC values of $16.2 \times 10^{-6} \text{ }^\circ\text{C}^{-1}$ at 25–570 °C and $30.6 \times 10^{-6} \text{ }^\circ\text{C}^{-1}$ at 570–900 °C, and an average TEC of $24.1 \times 10^{-6} \text{ }^\circ\text{C}^{-1}$ was calculated over the whole temperature range of 25–900 °C. These TEC values, especially at the high temperatures, are far beyond TECs, $(11\text{--}13) \times 10^{-6} \text{ }^\circ\text{C}^{-1}$, of the commonly used electrolyte materials in IT-SOFC,^[11–13] which is disadvantageous for structure and performance stability of the SOFCs. In contrast, LFCuO showed an almost linear expansion curve similar to other Fe–Cu-based perovskite oxides,^[28–30] giving rise to a much smaller TEC value of $12.0 \times 10^{-6} \text{ }^\circ\text{C}^{-1}$ at 25–900 °C. This TEC value is remarkably small compared to the TECs ($> 20 \times 10^{-6} \text{ }^\circ\text{C}^{-1}$) of cobalt-based perovskite oxides,^[7,31] and it is even smaller than the TEC results of Fe–Cu-based perovskite oxides such as $\text{La}_{0.5}\text{Sr}_{0.5}\text{Fe}_{0.8}\text{Cu}_{0.2}\text{O}_{3-\delta}$ ($17.7 \times 10^{-6} \text{ }^\circ\text{C}^{-1}$ at 25–900 °C),^[28] $\text{Nd}_{0.5}\text{Sr}_{0.5}\text{Fe}_{0.8}\text{Cu}_{0.2}\text{O}_{3-\delta}$ ($14.7 \times 10^{-6} \text{ }^\circ\text{C}^{-1}$ at 25–800 °C),^[32] and $\text{Ln}_{0.5}\text{Sr}_{0.5}\text{Fe}_{0.8}\text{Cu}_{0.2}\text{O}_{3-\delta}$ ($\text{Ln}=\text{La}, \text{Pr}$ and Nd , $\text{TEC} \approx 16 \times 10^{-6} \text{ }^\circ\text{C}^{-1}$ at 30–850 °C).^[33] Most significantly, this TEC value matches perfectly with the TECs of electrolytes $\text{Ce}_{0.8}\text{Sm}_{0.2}\text{O}_{1.9}$ (SDC) and $\text{Ce}_{0.8}\text{Gd}_{0.2}\text{O}_{1.9}$ (GDC). As a result, structural stability of SOFCs can be expected when LFCuO is used as the cathode.

With the exception of the excellent TEC matching of LFCuO with electrolytes from an application point of view, the exact reasons for the dramatically different TEC values between LFCuO and BFCuO are also intriguing and worthy of further investigation. It is known that two factors are related to the thermal expansion behaviors of the perovskite oxides: one is “chemical expansion” induced by reduction and spin transition of the B-site ions and the other is “crystal expansion” from anharmonic atomic vibrations that depend on electrostatic attraction forces within the lattice.^[27,34,35] Co-based perovskite oxides usually show large TEC values above $20 \times 10^{-6} \text{ }^\circ\text{C}^{-1}$, mainly owing to the “chemical expansion” induced by the easily reduced Co^{n+} ($n=4,3$) ions at high temperatures as well

as the low-to-high spin transition of Co^{3+} .^[7,11] Therefore, partial or total replacement of cobalt ions with other transition-metal ions with relatively stable valences such as Fe, Cu, or Ni ions generally results in lower TEC values.^[11,36,37] However, the TEC values of perovskite oxides also change with the A-site cations when the B-site ions are kept the same. As typical examples, the average TEC value is $27.1 \times 10^{-6} \text{ }^\circ\text{C}^{-1}$ for $\text{Ba}_{0.5}\text{Sr}_{0.5}\text{Fe}_{0.8}\text{Cu}_{0.2}\text{O}_{3-\delta}$,^[38] whereas they are as low as 13.1×10^{-6} and $14.7 \times 10^{-6} \text{ }^\circ\text{C}^{-1}$ for $\text{Bi}_{0.5}\text{Sr}_{0.5}\text{Fe}_{0.8}\text{Cu}_{0.2}\text{O}_{3-\delta}$ ^[29] and $\text{Nd}_{0.5}\text{Sr}_{0.5}\text{Fe}_{0.8}\text{Cu}_{0.2}\text{O}_{3-\delta}$,^[32] respectively, in similar measurement temperature ranges. Similarly, different A-site cations, La^{3+} and Ba^{2+} , also caused dramatically different TEC values for LFCuO ($12.0 \times 10^{-6} \text{ }^\circ\text{C}^{-1}$) and BFCuO ($24.1 \times 10^{-6} \text{ }^\circ\text{C}^{-1}$) in this work. It was reported^[34] that $V_{\text{O}}^{\bullet\bullet}$ in perovskite oxides could induce a reduction in the electrostatic bond strength of the lattice and increase “crystal expansion” in the oxides, whereas the concentration of $V_{\text{O}}^{\bullet\bullet}$ in the oxide is closely associated with the valence states and contents of the A-site cations. This is probably the reason for the changing TECs with different A-site cations in the oxides. A further interpretation of the different TEC values for LFCuO and BFCuO is given in the following part, based on the results of the oxygen content and chemical defects.

2.3. Oxygen Content and Chemical Defects

To get a deeper understanding of the different TEC values for LFCuO and BFCuO, and for interpretation of the electrical and electrochemical properties, the oxygen content ($3-\delta$), oxygen deficiency (δ , that is, content of $V_{\text{O}}^{\bullet\bullet}$), and average valence (n) of Fe^{n+} ions in the as-synthesized LFCuO and BFCuO oxides were measured by using the iodometric titration method at room temperature, and the results are listed in Table 1. It is found that the oxygen content (2.60) of BFCuO is much lower than that (2.98) of LFCuO; thus, BFCuO has a much higher oxygen deficiency ($\delta=0.40$) than that of LFCuO ($\delta=0.020$). This is probably because the high-valence La^{3+} ions need more O^{2-} ions than the lower valence Ba^{2+} ions to maintain electroneutrality of the oxide. The average valence of Fe^{n+} ions in the oxides is $3 < n < 4$, indicating that both Fe^{4+} and Fe^{3+} ions existed at B sites of the oxides.

Temperature-dependence of $3-\delta$ and δ for both oxides was further calculated based on the thermogravimetric (TG) results (Figures 3 and 4), which gave the weight change of the oxides as a function of temperature. As shown in Figure 3 a, a gradual weight decrease occurred at higher temperatures in LFCuO and a 0.45 wt% decrease was found at 800 °C. This weight loss was attributed to thermal-driven release of the lattice oxygen; therefore, a gradual decrease in oxygen content and increase in oxygen deficiency with higher temperatures followed (Figures 3 b and 3 c) and the oxygen deficiency in LFCuO is 0.087 at 800 °C. In the case of BFCuO, however, a different TG curve was obtained (Figure 4 a): a slight weight gain (0.15 wt%) first occurred in the low-temperature range of 340–460 °C, which could be ascribed to an oxygen-adsorption process as found in other perovskite oxides.^[33,39] This process happened in BFCuO, but not in LFCuO, possibly because the as-synthesized BFCuO

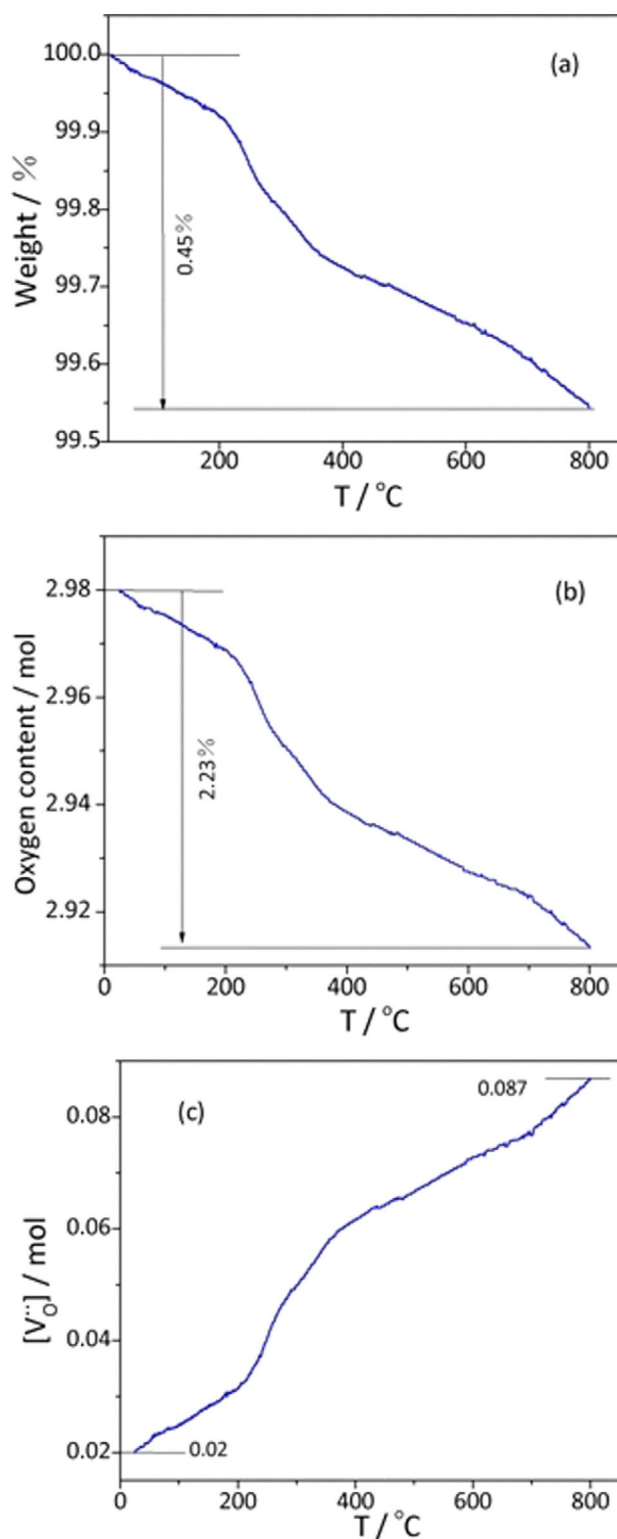


Figure 3. a) TG curve, b) oxygen content, and c) content of V_{O}^{**} as a function of temperature for LFCuO.

had a very large oxygen deficiency. Besides, as shown in Figure 4b, a 5.82 mol% decrease in oxygen content of BFCuO was found at 800 °C, which was much larger than that of LFCuO (2.23 mol%), indicating that the lattice oxygen in BFCuO was more easily released than in LFCuO. As a result, a

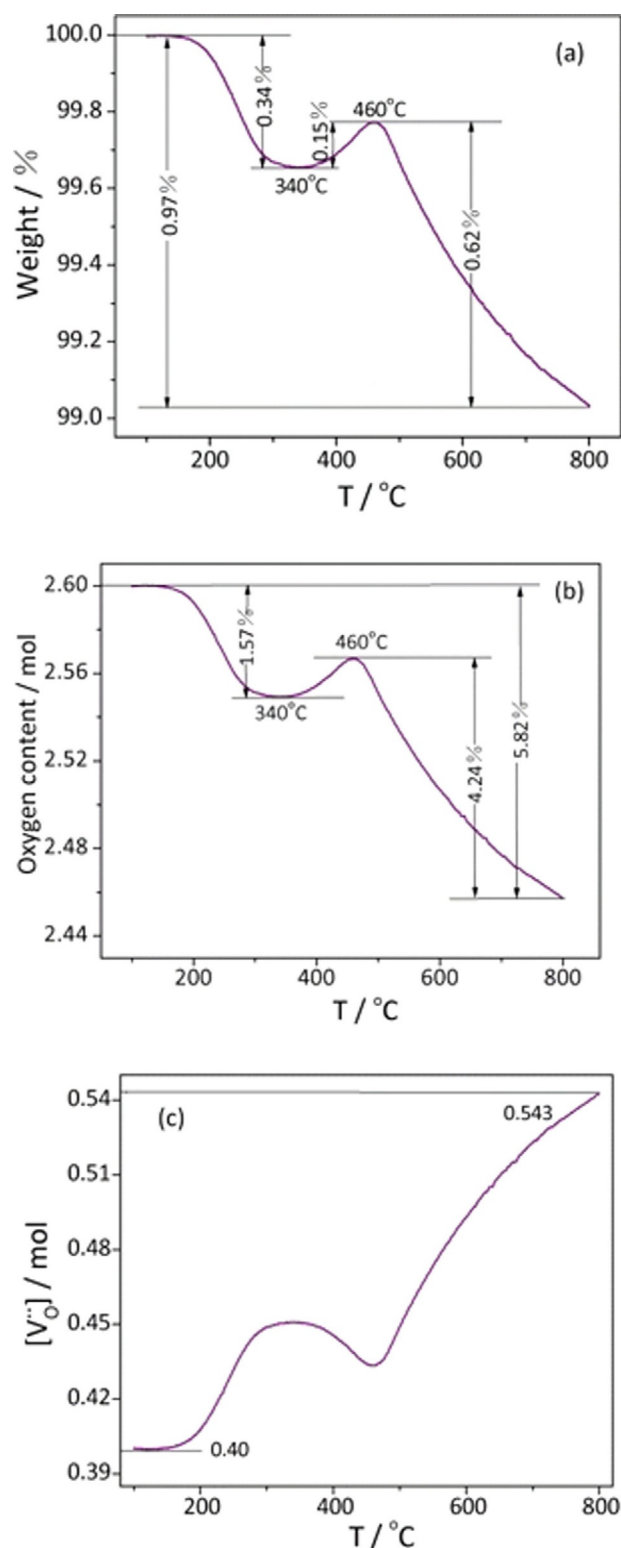


Figure 4. a) TG curve, b) oxygen content, and c) content of V_{O}^{**} as a function of temperature for BFCuO.

very high oxygen deficiency (0.543) was obtained at 800 °C for BFCuO (Figure 4c), which is about five times as high as that of LFCuO (0.087).

Given the above results, we could go back to the significantly larger TEC value for BFCuO compared to LFCuO (Figure 2). In

BFCuO, more lattice oxygen was released at high temperatures than in LFCuO; therefore, more B-site $\text{Fe}^{4+}/\text{Fe}^{3+}$ ions could be reduced to $\text{Fe}^{3+}/\text{Fe}^{2+}$ and then “chemical expansion” was promoted. Besides, as $V_{\text{O}}^{\bullet\bullet}$ could reduce electrostatic bond strength in perovskite oxides,^[34] higher concentration of $V_{\text{O}}^{\bullet\bullet}$ (i.e. larger oxygen deficiency) could enhance the “crystal expansion” and then increase the TEC value of BFCuO as well. Song and Lee^[38] found that the Co-free perovskite oxide $\text{Ba}_{0.5}\text{Sr}_{0.5}\text{Cu}_{0.2}\text{Fe}_{0.8}\text{O}_{3-\delta}$ had an “abnormally” large TEC value ($27.1 \times 10^{-6} \text{ }^{\circ}\text{C}^{-1}$) compared to the Co-containing oxide $\text{Ba}_{0.5}\text{Sr}_{0.5}\text{Co}_{0.2}\text{Fe}_{0.8}\text{O}_{3-\delta}$ ($16.5 \times 10^{-6} \text{ }^{\circ}\text{C}^{-1}$) at 100–800 °C, which was ascribed to the much larger oxygen deficiency in the former oxide. Similarly, the large oxygen deficiency in BFCuO could also have played an important role in the large TEC value.

2.4. Electrical Conductivities

The total electrical conductivities of BFCuO and LFCuO were measured in the temperature range of 300–800 °C in air, and the results are present in Figure 5. With increasing tempera-

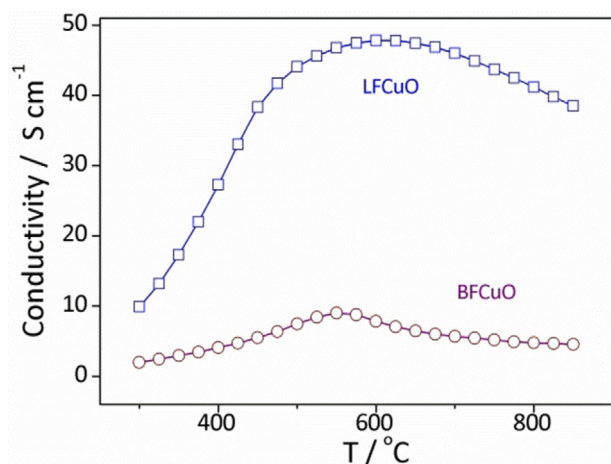


Figure 5. Temperature dependence of electrical conductivity for BFCuO and LFCuO, measured in air.

ture, the conductivity values of both oxides first increased and then decreased after reaching a maximum point, indicating an insulator-to-metal conduction transition that is typical of the perovskite-type mixed ionic–electronic conductors (MIECs).^[7]

For these MIEC systems, the total electrical conductivity is dominated by the electronic conduction (p-type semiconductor), which occurs through a Zerner mechanism^[7,40] with electronic hopping along the pathway of $-\text{M}^{n+}-\text{O}^{2-}-\text{M}^{(n+1)+}$ (where M is a transition-metal ion with changeable valence at B sites of the oxides like Fe in BFCuO and LFCuO). Therefore, conductivities of the MIEC oxides are intrinsically determined by the concentration and mobility of the charge carriers (h^{\bullet}) and also influenced by existence of $V_{\text{O}}^{\bullet\bullet}$ in the lattice, as $V_{\text{O}}^{\bullet\bullet}$ can break the electronic hopping pathway and decrease the electronic mobility.^[7] Similar to other perovskite-type MIECs, the increasing electrical conductivity in the low-temperature

range for BFCuO and LFCuO could be attributed to the thermal activation of electronic hopping, and the gradually decreasing conductivity at the high temperatures was caused by the decreasing concentration of charge carriers h^{\bullet} as well as generation of $V_{\text{O}}^{\bullet\bullet}$ with the release of lattice oxygen.

BFCuO and LFCuO had the same electrical conduction mechanisms; however, their electrical conductivity values were quite different. The total conductivities of LFCuO ranged from 10.0 S cm^{-1} at 300 °C to 41.2 S cm^{-1} at 800 °C, which were much higher than the conductivity values ($< 9.0 \text{ S cm}^{-1}$) of BFCuO. This difference in electrical conductivity is closely associated with their different chemical defects. As discussed above (Figures 3 and 4), BFCuO had a much higher concentration of $V_{\text{O}}^{\bullet\bullet}$ than LFCuO, and $V_{\text{O}}^{\bullet\bullet}$ could break the electronic hopping pathway and, thereby, decrease the electrical conductivity of BFCuO. Besides, $V_{\text{O}}^{\bullet\bullet}$ was generated through thermally driven release of lattice oxygen (O_2^{\times}) in the oxides based on the redox reaction of $\text{O}_2^{\times} + 2h^{\bullet} \rightarrow V_{\text{O}}^{\bullet\bullet} + \frac{1}{2}\text{O}_2$. With more $V_{\text{O}}^{\bullet\bullet}$ formed in BFCuO, more charge carriers h^{\bullet} were consumed, which could also decrease the conductivities of BFCuO.

2.5. Chemical Compatibility

Chemical compatibility between component materials at high temperatures is necessary for long-term performance stability of SOFCs. To check the chemical compatibility of BFCuO and LFCuO with electrolytes, LFCuO–SDC/GDC and BFCuO–SDC/GDC mixed powders in 1:1 weight ratios were calcined at different temperatures between 900 and 1000 °C for 10 h in air, and then XRD patterns were measured at room temperature. The obtained XRD patterns are shown in Figure 6. It can be observed in Figure 6a that the XRD pattern of the LFCuO–SDC mixture was composed of LFCuO and SDC individual phases and no new diffraction peaks were found; thus, no reaction occurred between LFCuO and SDC at 1000 °C. In contrast, in the XRD pattern of the BFCuO–SDC mixture, besides the diffraction peaks from the BFCuO and SDC individual phases, some minor diffraction peaks ascribed to an impurity phase of $\text{Ba}_6\text{SmCu}_3\text{O}_{10.96}$ (ICSD 80-1879) were also observed, demonstrating a chemical reaction between BFCuO and SDC at 900 °C. Similar results were also obtained with the electrolyte of GDC (Figure 6b): LFCuO did not react with GDC at 1000 °C, but an additional phase was formed in the BFCuO–GDC mixture calcined at 900 °C, owing to a reaction between BFCuO and GDC. These results have demonstrated that LFCuO has better high-temperature chemical compatibility with SDC and GDC than BFCuO.

2.6. Electrochemical Performance

To avoid a chemical reaction between the cathode and the electrolyte, the BFCuO cathode layer can not be calcined at temperatures above 900 °C on SDC or GDC electrolyte pellets. So, a calcination temperature of 890 °C was tried for the fabrication of a symmetric cell: BFCuO/SDC/BFCuO. However, poor connection between the cathode and electrolyte layers was found at this temperature and the BFCuO cathode layer easily

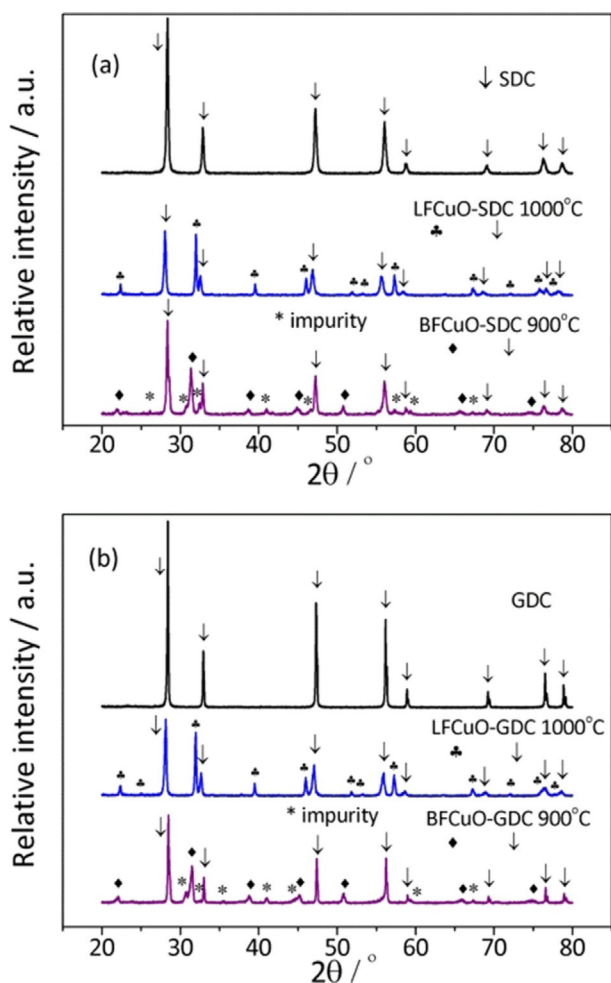


Figure 6. XRD patterns of a) the LFCuO–SDC and BFCuO–SDC mixed powders and of b) the LFCuO–GDC and BFCuO–GDC mixed powders calcined at 1000 and 900 °C, respectively, for 10 h in air.

peeled off from the electrolyte pellet. Therefore, the electrochemical performance of the BFCuO cathode could not be further studied. In contrast, as LFCuO was chemically stable with GDC and SDC at temperatures up to 1000 °C, a calcination temperature of 950 °C was adopted for the fabrication of the LFCuO cathode layer. At this temperature, a good cathode/electrolyte connection was obtained, as indicated by the cross-sectional SEM image of the LFCuO/SDC/LFCuO symmetrical cell (Figure 7a). This interface connection is advantageous for interfacial transfer of oxygen ions with low interface resistances. Besides, the fabricated LFCuO cathode layer had uniformly porous microstructure with well-linked grains of approximately 300 nm in size (Figure 7b), which could realize continuous electronic and ionic transportation and easy gas diffusion in the cathode.

AC impedance spectra of the symmetric cell LFCuO/SDC/LFCuO were measured at 650–800 °C in air (Figure 8a). The ohmic resistances (intercepts at the high frequency with the real axis) arising from the electrolyte and lead wires were normalized to zero for clarity. The frequencies for these EIS plots are in the range of approximately 10⁴–0.1 Hz. The intercepts of the arc at the highest and lowest frequencies in the spectra

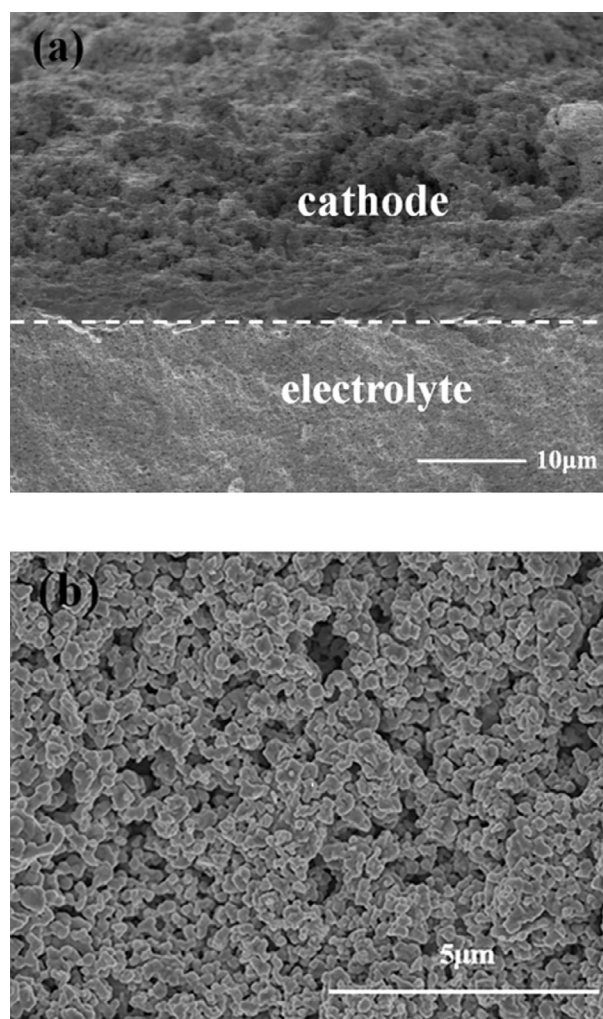


Figure 7. a) Cross-sectional and b) surface SEM images of the symmetric cell of LFCuO/SDC/LFCuO.

relate to the polarization resistance (R_p) from both identical cathodes, so area-specific resistance (ASRs) of one cathode can be calculated by using $ASR = 1/2R_pS$, where S is area of the cathode. The obtained ASR results were inserted in Figure 8a and are shown in the Arrhenius plot in Figure 8b. According to the slope of the Arrhenius plot, the reaction activation energy (E_a) of the LFCuO cathode was calculated to be 1.65 eV, which is similar to E_a values of other Fe–Cu-based perovskite cathodes.^[33] The ASR values of the LFCuO cathode are 0.09 Ωcm^2 at 800 °C, 0.20 Ωcm^2 at 750 °C, 0.55 Ωcm^2 at 700 °C, and 1.6 Ωcm^2 at 650 °C. These ASRs of LFCuO are comparable to, if not smaller than, ASRs of many other Fe–Cu-based perovskite cathodes, such as $\text{Pr}_{0.5}\text{Sr}_{0.5}\text{Fe}_{0.8}\text{Cu}_{0.2}\text{O}_{3-\delta}$ (1.25 Ωcm^2 at 700 °C),^[41] $\text{La}_{0.8}\text{Sr}_{0.2}\text{Fe}_{0.8}\text{Cu}_{0.2}\text{O}_{3-\delta}$ (0.58 Ωcm^2 at 750 °C and 0.31 Ωcm^2 at 800 °C),^[14] and $\text{SmBa}_{0.5}\text{Sr}_{0.5}\text{CuFeO}_{5+\delta}$ (0.28 Ωcm^2 at 750 °C).^[42] Smaller polarization resistances indicate higher ORR catalytic activity, which, together with the significantly low TEC value (Figure 2) that matches with TEC of electrolytes, have demonstrated that LFCuO is a promising new cobalt-free perovskite cathode for IT-SOFCs.

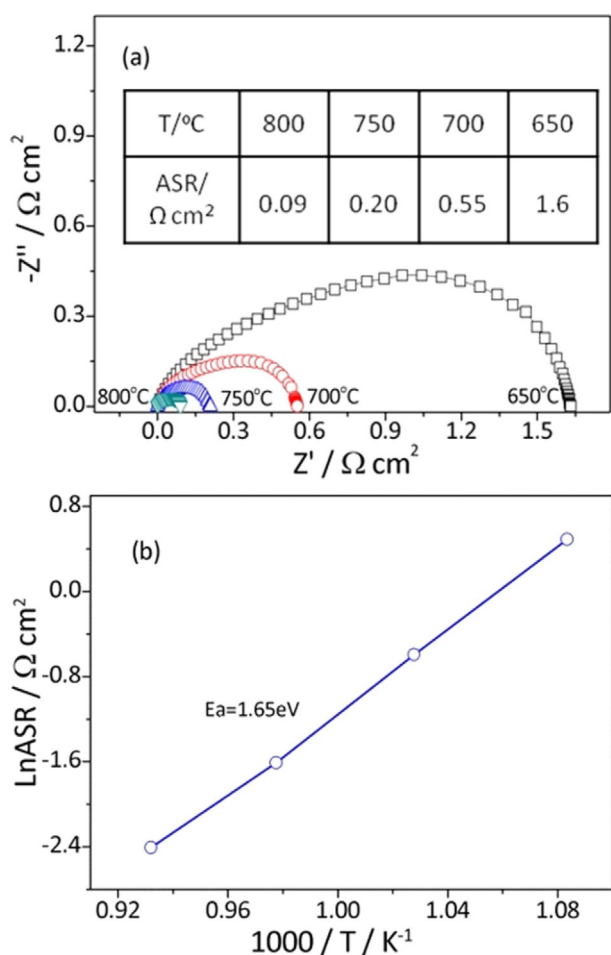


Figure 8. a) AC impedance spectra of the symmetric cell of LFCuO/SDC/LFCuO measured at 650–800 °C in air with the inserted ASR results; b) Arrhenius plot of the ASR data at different temperatures.

3. Conclusions

In this work, two new cobalt-free perovskite oxides, LFCuO and BFCuO, were synthesized and studied as cathode materials of SOFCs in comparison. BFCuO had a $Pm-3m$ cubic perovskite structure, whereas LFCuO presented an orthorhombically distorted perovskite structure. The different phase structures were attributed to their different tolerance factors with different cations (Ba^{2+} and La^{3+}) at the A sites. BFCuO had a very large TEC value ($24.1 \times 10^{-6} \text{ }^\circ\text{C}^{-1}$) at 25–900 °C. In contrast, the TEC value of LFCuO, $12.0 \times 10^{-6} \text{ }^\circ\text{C}^{-1}$, was remarkably low and perfectly matched with TECs of commonly used electrolyte materials. The combined “chemical expansion” and “crystal expansion” resulted in the large TEC of BFCuO. Electrical conductivities of LFCuO ranged from 10.0 S cm^{-1} at 300 °C to 42.0 S cm^{-1} at 800 °C, which are higher than conductivities of BFCuO. These different properties for LFCuO and BFCuO were closely associated with their different oxygen content and chemical defects. Moreover, LFCuO was chemically stable with SDC and GDC electrolytes at 1000 °C in air, whereas BFCuO reacted with them at 900 °C. The low inter-reaction temperature for BFCuO and SDC/GDC made it impossible to fabricate the

symmetric cell for impedance spectra measurements. In contrast, a symmetric cell was successfully fabricated based on the LFCuO cathode, and ASRs of LFCuO were determined to be $0.090 \text{ } \Omega \text{ cm}^2$ at 800 °C, $0.20 \text{ } \Omega \text{ cm}^2$ at 750 °C, and $0.55 \text{ } \Omega \text{ cm}^2$ at 700 °C. These ASR values were smaller than the ASRs of some other Fe–Cu-based perovskite oxides, demonstrating high ORR catalytic activity of LFCuO. These results have demonstrated that LFCuO has much better overall performance than BFCuO and it is a new promising cobalt-free cathode material for IT-SOFCs.

Experimental Section

Experimental Details

Synthesis of the Powders

$\text{BaFe}_{0.8}\text{Cu}_{0.2}\text{O}_{3-\delta}$ (BFCuO) and $\text{LaFe}_{0.8}\text{Cu}_{0.2}\text{O}_{3-\delta}$ (LFCuO) powders were synthesized with an ethylene diamine tetraacetic acid (EDTA) complex sol-gel method, as described in our previous work.^[31,33] All the reagents used are of analytical reagent (AR) degree. The synthesis process was described as follows, taking LFCuO as an example. Firstly, stoichiometric amounts of $\text{Fe}(\text{NO}_3)_3 \cdot 9\text{H}_2\text{O}$, $\text{Cu}(\text{NO}_3)_2 \cdot 3\text{H}_2\text{O}$, and $\text{La}(\text{NO}_3)_3 \cdot 6\text{H}_2\text{O}$ were dissolved in EDTA– $\text{NH}_3 \cdot \text{H}_2\text{O}$ solution ($\text{pH} \approx 6$) whilst stirring to form an aqueous solution, and then citric acid– $\text{NH}_3 \cdot \text{H}_2\text{O}$ solution ($\text{pH} \approx 6$) was added at a mole ratio of 1:1:2 for EDTA/total metal ions/citric acid. The mixed solution was subsequently heated to 80 °C to obtain a dark dry foam structure, which was then decomposed on a hot plate to make the precursors, followed by calcination in air at 600 °C for 5 h and 800 °C for 2 h, in sequence. The precursor of LFCuO was finally calcined at 950 °C for 5 h to get a pure phase. The BFCuO and BaFeO_3 samples were synthesized with similar processes, but the final calcination temperature was 1050 °C. To check chemical reaction compatibility between the cathode and electrolyte materials, the LFCuO or BFCuO powders were, respectively, mixed with SDC or GDC electrolyte in a 50:50 weight ratio, followed by calcination at the temperatures of 900–1000 °C for 10 h in air.

Characterization

Phase structures of the as-synthesized LFCuO and BFCuO powders as well as the calcined LFCuO–SDC/GDC and BFCuO–SDC/GDC mixed powders were characterized by using X-ray diffraction measurements (XRD, Rigaku D/Max 2400). Thermal expansion data of LFCuO and BFCuO were collected with a dilatometer (Netzsch DIL 402PC) at 30–900 °C in air with a heating rate of $5 \text{ }^\circ\text{C min}^{-1}$. Oxygen contents ($3-\delta$) and average valences (n) of Fe^{n+} ions for LFCuO and BFCuO were determined by iodometric titrations^[43] at room temperature with blank tests and five parallel analyses to reduce the measurement error. TG analysis (Netzsch TG209F3) of the samples was carried out in a temperature range of 50–900 °C in air with heating rate of $5 \text{ }^\circ\text{C min}^{-1}$ to check their thermal-driven oxygen-release behaviors. Electrical conductivities of both samples were measured at 300–800 °C in air by using a DC four-electrode method. A Solartron 1260 frequency response analyzer combined with a Solartron 1287 potentiostat was used for EIS measurements of the symmetrical cell of LFCuO/SDC/LFCuO under open circuit voltage (OCV) conditions at 650–800 °C in air. In the symmetric cell, the SDC pellet was fabricated by dry-pressing, and was calcined at 1370 °C for 10 h in air; the LFCuO ink, prepared by mixing the cathode powders with α -terpineol and ethyl cellulose, was screen-

printed onto both sides of the SDC pellet and fired at 950 °C for 2 h in air.

Acknowledgements

This work was financially supported by the Fundamental Research Funds for the Central Universities (DUT18LAB06)^o, the National Key R & D Program of China (2017YFA0402501), and the Fundamental Research (Discipline Arrangement) project funding from Shenzhen Science and Technology Innovation Committee (Grant No. JCYJ20170412154554048).

Conflict of Interest

The authors declare no conflict of interest.

Keywords: chemical defects · oxygen reduction reaction · perovskite oxide · structure · thermal expansion

- [1] Z. Gao, L. V. Mogni, E. C. Miller, J. G. Railsback, S. A. Barnett, *Energy Environ. Sci.* **2016**, *9*, 1602.
- [2] R. A. Rincón, E. Ventosa, F. Tietz, J. Masa, S. Seisel, V. Kuznetsov, W. Schuhmann, *ChemPhysChem* **2014**, *15*, 2810.
- [3] Y. Zhu, W. Zhou, Z. Shao, *Small* **2017**, *13*, 1.
- [4] J. Nielsen, E. M. Skou, T. Jacobsen, *ChemPhysChem* **2015**, *16*, 1635.
- [5] B. Zhu, B. Wang, Y. Wang, R. Raza, W. Tan, J. S. Kim, P. A. van Aken, P. Lund, *Nano Energy* **2017**, *37*, 195.
- [6] M. Grünbacher, T. Götsch, A. K. Opitz, B. Klötzer, S. Penner, *ChemPhysChem* **2018**, *19*, 93.
- [7] S. B. Adler, *Chem. Rev.* **2004**, *104*, 4791.
- [8] Y. L. Yang, A. J. Jacobson, C. L. Chen, G. P. Luo, K. D. Ross, C. W. Chu, *Appl. Phys. Lett.* **2001**, *79*, 776.
- [9] A. Tarancón, M. Burriel, J. Santiso, S. J. Skinner, J. A. Kilner, *J. Mater. Chem.* **2010**, *20*, 3799.
- [10] S. Pang, X. Jiang, X. Li, Z. Su, H. Xu, Q. Xu, C. Chen, *Int. J. Hydrogen Energy* **2012**, *37*, 6836.
- [11] J. H. Kim, A. Manthiram, *Electrochim. Acta* **2009**, *54*, 7551.
- [12] J. Xue, Y. Shen, T. He, *J. Power Sources* **2011**, *196*, 3729.
- [13] W. Zajac, K. Świerczek, J. Molenda, *J. Power Sources* **2007**, *173*, 675.
- [14] F. Zurlo, E. Di Bartolomeo, A. D'Epifanio, V. Felice, I. Natali Sora, L. Tortora, S. Licocchia, *J. Power Sources* **2014**, *271*, 187.
- [15] F. Dong, Y. Chen, D. Chen, Z. Shao, *ACS Appl. Mater. Interfaces* **2014**, *6*, 11180.
- [16] S. Vázquez, L. Suescun, R. Faccio, *J. Power Sources* **2016**, *311*, 13.
- [17] J. F. Basbus, F. D. Prado, A. Caneiro, L. V. Mogni, *J. Electroceram.* **2014**, *32*, 311.
- [18] F. Dong, D. Chen, Y. Chen, Q. Zhao, Z. Shao, *J. Mater. Chem.* **2012**, *22*, 15071.
- [19] J. Wang, K. Y. Lam, M. Saccoccio, Y. Gao, D. Chen, F. Ciucci, *J. Power Sources* **2016**, *324*, 224.
- [20] J. Wang, M. Saccoccio, D. Chen, Y. Gao, C. Chen, F. Ciucci, *J. Power Sources* **2015**, *297*, 511.
- [21] C. Zhu, X. Liu, D. Xu, D. Yan, D. Wang, W. Su, *Solid State Ionics* **2008**, *179*, 1470.
- [22] X. Jiang, J. Wang, G. Jia, Z. Qie, Y. Shi, A. Idrees, Q. Zhang, L. Jiang, *Int. J. Hydrogen Energy* **2017**, *42*, 6281.
- [23] C. A. L. Dixon, C. M. Kavanagh, K. S. Knight, W. Kockelmann, F. D. Morrison, P. Lightfoot, *J. Solid State Chem.* **2015**, *230*, 337.
- [24] P. M. Woodward, *Acta Crystallogr. Sect. B* **1997**, *53*, 44.
- [25] V. M. Goldschmidt, *Naturwissenschaften* **1926**, *14*, 477.
- [26] E. V. Tsipis, M. V. Patrakeev, V. V. Kharton, A. A. Yaremchenko, G. C. Mather, A. L. Shaula, I. A. Leonidov, V. L. Kozhevnikov, J. R. Frade *Solid State Sci.* **2005**, *7*, 355.
- [27] I. Kaus, H. U. Anderson, *Solid State Ionics* **2000**, *129*, 189.
- [28] J. Lu, Y. M. Yin, J. Li, L. Xu, Z. F. Ma, *Electrochem. commun.* **2015**, *61*, 18.
- [29] L. Gao, M. Zhu, Q. Li, L. Sun, H. Zhao, J.-C. Grenier, *J. Alloys Compd.* **2017**, *700*, 29.
- [30] Q. Zhou, L. Xu, Y. Guo, D. Jia, Y. Li, W. C. J. Wei, *Int. J. Hydrogen Energy* **2012**, *37*, 11963.
- [31] S. L. Pang, X. N. Jiang, X. N. Li, H. X. Xu, L. Jiang, Q. L. Xu, Y. C. Shi, Q. Y. Zhang, *J. Power Sources* **2013**, *240*, 54.
- [32] J.-W. Yin, Y.-M. Yin, J. Lu, C. Zhang, N. Q. Minh, W. Zhang, Z.-F. Ma, *Int. J. Hydrogen Energy* **2014**, *39*, 17852.
- [33] S. Pang, W. Wang, T. Chen, X. Shen, Y. Wang, K. Xu, X. Xi, *J. Power Sources* **2016**, *326*, 176.
- [34] W. Zhou, R. Ran, Z. Shao, W. Jin, N. Xu, *J. Power Sources* **2008**, *182*, 24.
- [35] F. Dong, Y. Chen, R. Ran, D. Chen, M. O. Tade, S. Liu, Z. Shao, *J. Mater. Chem. A* **2013**, *1*, 9781.
- [36] X. Li, X. Jiang, S. Pang, Q. Wang, Z. Su, Q. Zhang, *Int. J. Hydrogen Energy* **2011**, *36*, 13850.
- [37] Y. N. Kim, J. H. Kim, A. Manthiram, *J. Power Sources* **2010**, *195*, 6411.
- [38] K.-W. Song, K.-T. Lee, *Ceram. Int.* **2012**, *38*, 5123.
- [39] C. Frontera, A. Caneiro, A. E. Carrillo, J. Oró-Solé, J. L. García-Muñoz, *Chem. Mater.* **2005**, *17*, 5439.
- [40] P. Zeng, R. Ran, Z. Chen, W. Zhou, H. Gu, Z. Shao, S. Liu, *J. Alloys Compd.* **2008**, *455*, 465.
- [41] C. G. Moura, J. P. de F. Grilo, D. A. Macedo, M. R. Cesário, D. P. Fagg, R. M. Nascimento, *Mater. Chem. Phys.* **2016**, *180*, 256.
- [42] X. Ding, X. Kong, H. Wu, Y. Zhu, J. Tang, Y. Zhong, *Int. J. Hydrogen Energy* **2012**, *37*, 2546.
- [43] E. Rautama, P. Boullay, A. K. Kundu, V. Caignaert, V. Pralong, M. Karppinen, B. Raveau, *Chem. Mater.* **2008**, *20*, 2742.

Received: May 28, 2018